Rotation capacity of beams prestressed with synthetic external tendons

CLAUDIA CAMPOS
Dept. of Civil Engineering, Military Institute of Engineering, Rio de Janeiro, Brazil
GIUSEPPE GUIMARÃES
Dept. of Civil Engineering, Pontifical Catholic University of Rio de Janeiro, Brazil
CHRIS BURGOYNE
Dept. of Engineering, University of Cambridge, Cambridge, UK

ABSTRACT
The paper describes a numerical parametrical study of the flexural resistance of concrete beams prestressed with external parallel-lay aramid ropes with particular emphasis on the rotation capacity of a critical section. A relationship between the rotation capacity and the relative position of the neutral axis is proposed and comparisons between numerical predictions and experimental data show good agreement. The results highlight the implications of considering tendons with different moduli of elasticity. It is also shown that the proposed relationship can be applied to a rigid-plastic model for predicting the ultimate force in unbonded tendons.

INTRODUCTION
External prestressing techniques have been used both in new structures and in rehabilitation of existing ones. Some advantages of this technique are the possibility of controlling and adjusting the tendon forces, the ability to inspect, replace and add tendons, and lower weight. To overcome problems due to corrosion of steel, the non-corrodable nature of parallel-lay ropes, made of aramid fibres, makes them suitable for external prestressing applications. Experimental works (Formagini 1999; Araújo, 1997; Branco, 1993) and the recent construction of a bridge (Kherkof, 1998) have demonstrated the viability of aramid ropes as external prestressing tendons.

Aramid tendons exhibit a linear behaviour up to failure with no plasticity, and a lower modulus of elasticity than steel. Despite the difference in the prestressing material, the overall behaviour of beams prestressed with external tendons is similar, with the final failure given by concrete crushing in the compression zone at a particular section, leading to a complete collapse of the structure (Burgoyne et.al., 1991). In the loading regime before concrete cracking, the behaviour of beams shows no difference between those prestressed with aramid tendons and those prestressed with steel. After concrete cracking, however, the beams show a sudden increase in their deflections; the tendon modulus influences the flexibility, ultimate load and final rotation capacity of the beams, because of the different development of tendon force in the post-cracking range.

This paper focuses on a numerical parametrical study of the flexural resistance of concrete beams prestressed with external parallel-lay aramid ropes, with particular emphasis on the

FRPRCS-5, Thomas Telford, London, 2001.

rotation capacity of a critical section. A relationship between the rotation capacity and the relative position of the neutral axis is proposed. The results highlight the effects of different moduli of elasticity of tendons on the behavior of the beams. The comparison between numerical predictions and experimental results shows good agreement. It is also concluded that the proposed relationship can be applied to a rigid-plastic model for predicting the ultimate force in unbonded tendons.

NUMERICAL PARAMETRICAL STUDY

Campos (1999) carried out a numerical parametrical study of the flexural resistance of concrete beams prestressed with external tendons, with particular emphasis on prestressing with parallel-lay aramid tendons. A computer program based on the finite element method was used (Campos, 1993).

The finite element program analyses reinforced or prestressed concrete structures with either bonded or unbonded tendons, including external prestressing. It takes into account material and geometrical non-linearities. The constitutive relationship for the concrete is that recommended by the CEB/FIP Model Code (1990); reinforcing steel, prestressing steel and aramid tendons are all included. The program allows for slip and friction at the deviators as the load increases. The non-linear equations can be solved either by Newton-Raphson or Displacement-Control methods. Several examples have been analysed and compared with experimental results of beams prestressed with unbonded internal and external steel or aramid tendons (Formagini, 1999; Araújo, 1997; Branco, 1993; Guimarães, 1988). These comparisons have shown that the model can predict with good accuracy the overall behaviour and failure mode of such beams (Figure 1).

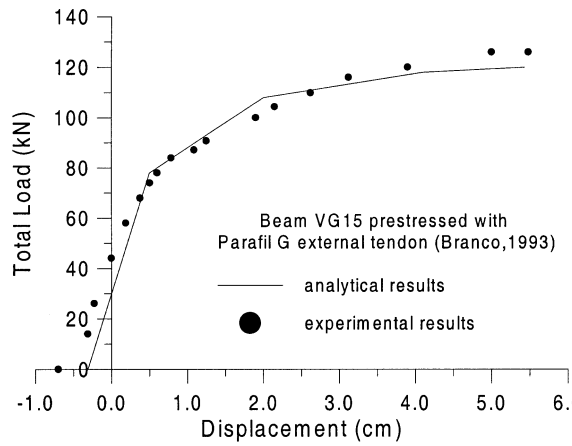

Figure 1. Typical comparison between experimental and analytical results for a beam prestressed with external parallel-lay tendons.

The current parametric study was carried out considering monolithic and simply supported beams (Figure 2). The main variables considered were the span-depth ratio, total reinforcement index, concrete strength, initial prestressing stress, modulus of elasticity of prestressing tendon, cross-sectional shape and type of loading. The beams were divided into groups as shown in Table 1. The friction coefficient was taken as 0.32 for all groups (Guimarães, 1988) and two main variables were always considered: total reinforcement index and elastic modulus of the prestressing tendon. The prestressing reinforcement area and the steel reinforcement in the compression zone were

constant for all beams (A_p= 3.05 cm^2, A_S'= 0.63 cm^2, respectively). On the other hand, the steel reinforcement area in the tension zone (A_s) varied, leading to different values for a reinforcement parameter, ρ_t, defined by

$$\rho_t = \frac{A_p}{b_f d_p} + \frac{A_s}{b_f d_p} - \frac{A_s'}{b_f d_p} \tag{1}$$

where b_f is the flange width in the compression zone, and d_p is the distance from extreme compression fibre to the centre of prestressing tendon. A total reinforcement index was defined as

$$\omega_t = \frac{A_p}{b_f d_p}\frac{f_{pe}}{f_c} + \frac{A_s}{b_f d_p}\frac{f_y}{f_c} - \frac{A_s'}{b_f d_p}\frac{f_y}{f_c} \tag{2}$$

where f_{pe} and f_c are the initial prestressing stress and concrete strength, respectively. The reinforcement index given by equation 2, was derived from the equilibrium between compression and tension forces at a critical section. This parameter is related to the curvature and, consequently, with the depth of neutral axis at a section. In the analysis, this parameter varied in a range from 0.07 to 0.46.

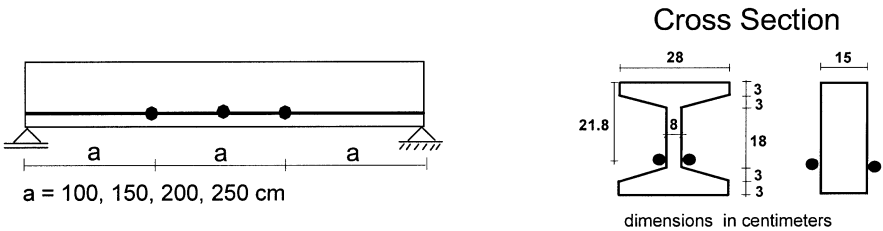

Figure 2. Layout of beams used in the parametric study.

Results

Figure 1 shows a typical load-displacement curve for beams prestressed with unbonded tendons. Moment-curvature and load-tendon force curves had the same pattern. Before concrete cracking, the behaviour of the beams was linear up to concrete cracking with no significant difference between the forces in the tendons with different moduli of elasticity, which is also confirmed by experimental results (Branco, 1993). After concrete cracking, the beams showed a sudden increase in their deflections, and two stages could be identified: the cracked-elastic and plastic stages.

The cracked-elastic stage was initiated after the first flexural cracks and the influence of the elastic modulus of the tendon, either in terms of displacements or force in the tendons, was not very significant. The transition to the plastic stage was characterised by yielding of the non-prestressed steel in the tension zone, with displacements, curvatures and force in the tendons increasing rapidly. Beams prestressed with aramid tendons showed higher rotation capacity than those prestressed with steel. The final failure was given by concrete crushing in

the compression zone at a particular section, even for those beams prestressed with a high initial prestressing stress.

Table 1. Details of the tested beams.
(Beams were tested with all combinations of tendon area and tendon material)

Group	f_c (MPa)	L/d_p	f_{pe}/f_{pu}	ρ_t	Cross Section	Type of loading	E_p (MPa)
A	43	13 20 27 34	0.55	0.0070 0.0102 0.0132 0.0181	I - Section	Third point load	200000 (steel) 123520 (Par. G) 77590 (Par. F)
B	43	13 20 27 34	0.25	0.0070 0.0102 0.0132 0.0181	I - Section	Third point load	200000 123520 77590
C	43	13 20 27 34	0.75	0.0070 0.0102 0.0132 0.0181	I - Section	Third point load	200000 123520 77590
D	70 43 30	20	0.55	0.0070 0.0102 0.0132 0.0181	I - Section	Third point load	200000 123520 77590
E	43	20	0.55	0.0070 0.0102 0.0132 0.0181	I - Section	Concentrated Load	200000 123520 77590
F	43	20	0.55	0.0115 0.0167 0.0215 0.0295	R - Section	Third point load	200000 123520 77590
G	43	20	0.55	0.0070 0.0102 0.0132 0.0181	I - Section	Third point load	200000 123520 77590

L/d_p = span-depth ratio; f_{pe} = initial prestressing stress; f_{pu} = tendon tensile strength
E_p = elastic modulus of the prestressing tendons
R - Section = Rectangular section
Par. G = Parafil Type G – aramid tendons with Kevlar 49 fibres
Par. F = Parafil Type F – aramid tendons with Kevlar 29 fibres

The effects of the variation of the tendon eccentricity were highlighted by the authors (Burgoyne et.al, 1996). If the tendon can move relative to the concrete, there can be a reduction in the lever arm of the tendon leading to reduction in load-carrying capacity. A comparative study on the effects of deviators at a critical section for the beams of group A was carried out. In the plastic stage, where significant loss of stiffness occurs, the results showed that this effect can be significant for beams with a span-depth ratio higher than 21, leading to a 70% reduction in the initial tendon eccentricity for the lowest value of reinforcement index. In addition, recent experimental results (Tan and Ng, 1997) confirmed the importance of preventing the movement of the tendon at critical sections.

Variables such as reinforcement area, concrete strength and initial prestressing force, which were considered in the reinforcement index term (equation 2) have a significant influence on the relative position of the neutral axis, $\xi = x/d_p$. Figure 3 shows the relationship between the relative position of the neutral axis and the total reinforcement index, ω_t, obtained from the numerical results for all groups of beams described in Table 1. These results were obtained by assuming that deviators were placed at midspan to avoid the effects of the eccentricity variation.

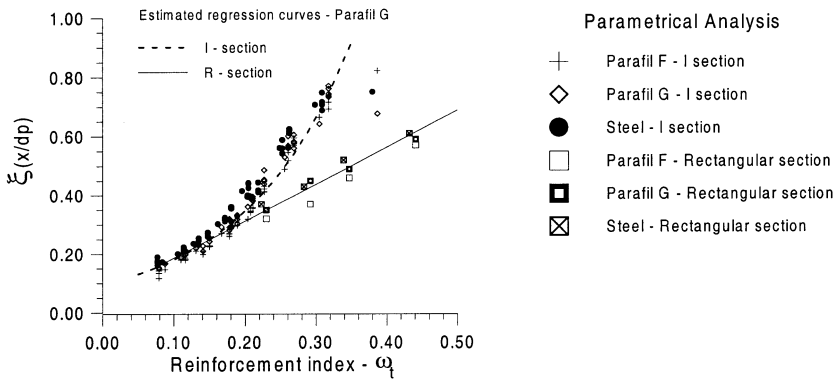

Figure 3. Relationship between relative position of the neutral axis (ξ) and total reinforcement index (ω_t), for beams from all groups.

The relationship between these two parameters was linear for beams with a rectangular section and for those with an I-section and a low value of the total reinforcement index, which meant that the neutral axis was localised in the flange. For I-section beams with high values of the reinforcement index, the neutral axis is located in the web, which leads to a non-linear relationship.

The elastic modulus of the tendons affected the relationship between the position of the neutral axis and the reinforcement index: the lower the elastic modulus, the lower was the parameter ξ due to a higher flexibility of the member. The following expressions, obtained by linear least squared analysis, were found to represent the relationship between total reinforcement index and the neutral axis position.

For rectangular sections

$$\begin{aligned} \xi_S &= 1.285\omega_t + 0.076 \quad (a) \quad \text{for } E_p = 195000 \text{ MPa} \\ \xi_G &= 1.256\omega_t + 0.060 \quad (b) \quad \text{for } E_p = 123520 \text{ MPa} \\ \xi_F &= 1.191\omega_t + 0.045 \quad (c) \quad \text{for } E_p = 77500 \text{ MPa} \end{aligned} \tag{3}$$

and for I sections,

$$\begin{aligned} \xi_S &= 0.110\, e^{6.26\omega_t} \quad (a) \quad \text{for } E_p = 195000 \text{ MPa} \\ \xi_G &= 0.094\, e^{6.5\omega_t} \quad (b) \quad \text{for } E_p = 123520 \text{ MPa} \\ \xi_F &= 0.0801\, e^{7.0\omega_t} \quad (c) \quad \text{for } E_p = 77500 \text{ MPa} \end{aligned} \tag{4}$$

A comparison between the estimated regression curves for beams with a rectangular section, given by equation 3(b), and the experimental results, given in Table 2, is made in Figure 4(a). The beams tested by Formagini (1999) had different concrete strengths, rectangular section and were prestressed with Parafil G tendons. The results showed a good agreement between the analytical curve and experimental data. The equation 4(b) for I section is plotted in Figure 4(b) together with the experimental data from Araújo (1997), Branco (1993) and Guimarães (1988) (Table 2). Reasonable agreement between the results can be seen but adjustments should be made for higher values of reinforcement index.

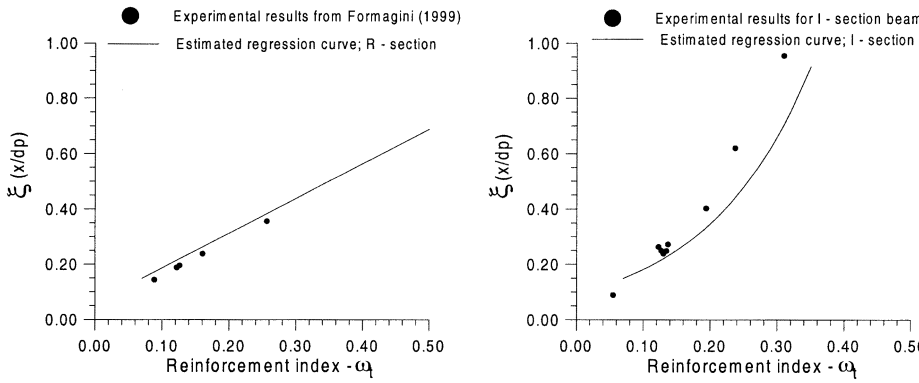

(a) (b)

Figure 4. Comparison between proposed curves and experimental data for beams prestressed with Parafil G tendons: (a) rectangular section; (b) I section.

The final rotation capacity of a member prestressed with unbonded tendons depends on the inelastic curvatures in the vicinity of the critical section at failure. The rotation capacity at failure can be expressed in terms of the parameter ξ as shown in Figure 5(a). The final rotation was strongly related to the main variables considered in the expression for the total reinforcement index, which influenced the parameter ξ. The results from the parametrical study also showed the influence of the span-depth ratio on the rotation capacity.

The full line plotted in Figure 5(a) is the estimated regression curve for beams with a span-depth ratio of 20. From these results, it can be seen that the influence of the elastic modulus of the prestressing tendons is accounted for by equations 3 and 4. The proposed relationships for values of span-depth ratio of 34, 27, 20 and 13 are given, respectively, by

$$\begin{aligned} \theta &= -0.008\ln(\xi) + 0.025 \quad \text{(a)} \\ \theta &= -0.011\ln(\xi) + 0.018 \quad \text{(b)} \\ \theta &= -0.012\ln(\xi) + 0.012 \quad \text{(c)} \\ \theta &= -0.010\ln(\xi) + 0.007 \quad \text{(d)} \end{aligned} \tag{5}$$

The efficiency of the proposed curve is demonstrated by a good agreement with the experimental results (Table 2) for beams prestressed with Parafil G and span-depth ratio of 20.6, as shown in Figure 5(b).

Note that the proposed curves (equations 5) are valid only for beams under third point loads, which had a higher rotation capacity than those subject to one concentrated load. The single point load leads to a short hinge that limits the plastic deformation near the critical section.

Table 2. Details of the beams tested by Formagini (1999); Araújo (1997); Branco (1993) e Guimarães (1988).

Group	Beam	Cross Section	Ep (MPa)	L/d_p	ω_t	ξ (exp)	θ_r(exp.) (rad)	Fps (exp.) (kN)
Formagini (1999)	VGR36	R section	123520	20.6	0.257	0.354	0.0182	352
	VGR57				0.161	0.237	0.0267	374
	VGR73				0.127	0.194	0.0283	394
	VGR74				0.122	0.187	0.0283	396
	VGR104				0.089	0.142	0.0295	410
Branco (1993)	VG10	I section	123520	13.5	0.123	0.262	0.0220	389
	VG15		123520	20.6	0.135	0.249	0.0270	379
	VG20		123520	27.5	0.128	0.248	0.0338	388
	VG25		123520	34.4	0.131	0.237	0.0370	379
	VF15		77750	20.6	0.137	0.271	0.0340	397
	VS15		195000	20.6	0.122	0.280	0.0229	378
Araújo (1997)	VG1	I section	123520	20.6	0.194	0.401	0.0200	348
	VG2				0.237	0.619	0.0147	331
	VG3				0.310	0.954	0.0154	335
Guimarães (1988)	VG1A	I section	123520	16	0.055	0.088	0.0244	743

VG = beams prestressed with Parafil G tendons ; VF = beams prestressed with Parafil F tendons; VS= beams prestressed with steel tendons; L/d_p = span-depth ratio; E_p = elastic modulus of the prestressing tendons; ω_t = total reinforcement index; ξ (exp) = experimental value for relative position of neutral axis; θ_r(exp.) = experimental value for rotation capacity; Fps (exp.) = experimental value for the final force in prestressing tendon.

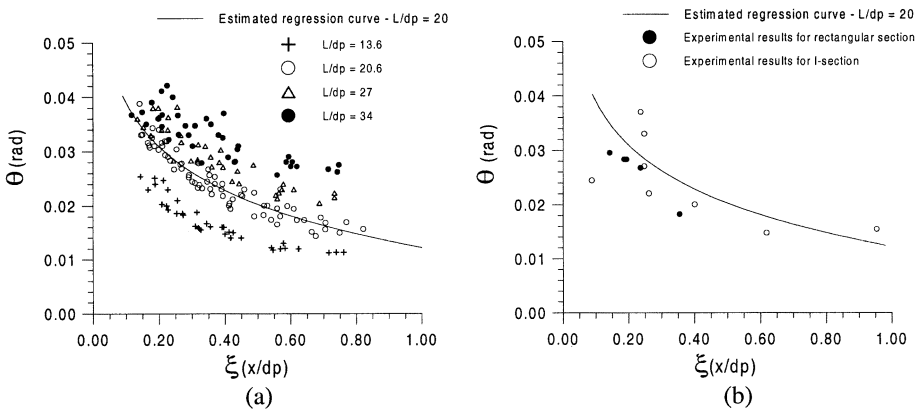

Figure 5. (a) Relationship between rotation capacity and position of the neutral axis: numerical data for beams with third point loading; (b) Comparison between proposed curve for rotation capacity and experimental results for beams data $L/d_p = 20.6$

PROPOSED CURVES AND RIGID PLASTIC ANALYSIS

The change in the force in an unbonded prestressing tendon depends on the overall behaviour of the beam rather than just the behaviour of one particular cross section. Slip at deviators, and the

eccentricity variation that occurs at a critical section, if the tendon can move relative to the concrete during loading, also affect the ultimate flexural resistance of these beams.

Tests on beams prestressed with external tendons have demonstrated that the failure mode is brittle and sudden, given by the concrete crushing, with the beam divided into a pair of rigid blocks as shown in Figure 6(a). In spite of this mode of failure, considerable rotation capacity is exhibited by these beams. Burgoyne et.al. (1996) proposed a simplified rigid plastic analysis of the failure mechanism of beams with unbonded tendons. The force in unbonded tendons can be predicted by taking into account the overall geometry of the beam, concrete strength and reinforcement index, as well as the effects of the friction at deviators. The main simplifying assumption is that all deformation takes place at a central hinge, which rotates about the neutral axis as shown in Figure 6(b). The neutral axis position is defined by the depth x which is a variable of the analysis and the rotation of the two blocks are both taken as θ.

These two parameters are initially unknown for the analysis of beams prestressed with unbonded tendons at the ultimate load. To solve this problem, it is necessary to relate axial displacement, that occurs in the compression failure zone, to axial strain of concrete. Data from Hillerborg (1990) were investigated by Campos (1999) in a rigid plastic analysis, but they did not produce a good agreement between numerical and experimental results. This is an important point which is currently being explored. On the other hand, the curves proposed here are close approximations for these two important parameters in the analysis of sections prestressed with unbonded tendons.

Table 3 shows the values obtained for the relative position of the neutral axis and the rotation capacity of a critical section, for all tested beams prestressed with external aramid tendons (and one prestressed with external steel tendons, VS15), using the proposed curves given by the set of equations 3, 4 and 5. These values were used in the rigid plastic analysis proposed by the authors (Burgoyne et.al., 1996; Campos, 1999). In general, a good correlation was found between numerical and experimental data either for rotation capacity, predicted by the proposed curves, or for final force in the prestressing tendons calculated using the rigid plastic analysis, as shown in Table 3.

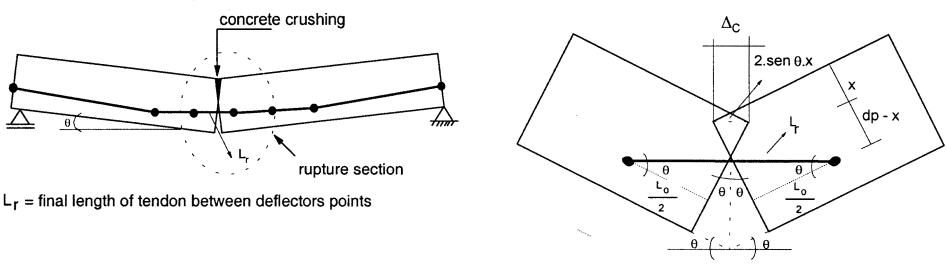

(a) (b)

Figure 6. (a) Deformed beam with central hinge at failure and (b) critical section in detail.

Table 3. Results for ξ and θ using proposed equations and final force in prestressing tendons using rigid plastic analysis.

Group	Beam	ω_t	ξ^*	θ^* (rad)	θ^*/θ(exp.)	Fps (num.)$^{\clubsuit}$ (kN)	Fps (num.)/ Fps(exp.)
Formagini (1999)	VGR36	0.257	0.38	0.023	1.264	405	1.151
	VGR57	0.161	0.26	0.027	1.011	381	1.019
	VGR73	0.127	0.22	0.030	1.060	406	1.030
	VGR74	0.122	0.21	0.030	1.060	404	1.025
	VGR104	0.089	0.17	0.033	1.119	420	1.024
Branco (1993)	VG10	0.123	0.21	0.021	0.955	395	1.015
	VG15	0.135	0.22	0.030	1.111	384	1.013
	VG20	0.128	0.22	0.034	1.006	388	1.000
	VG25	0.131	0.22	0.036	0.973	375	0.989
	VF15	0.137	0.20	0.031	0.912	365	0.919
	VS15	0.122	0.23	0.029	1.266	427	1.130
Araújo (1997)	G1	0.194	0.33	0.025	1.250	368	1.057
	G2	0.237	0.44	0.022	1.497	352	1.063
	G3	0.310	0.71	0.016	1.039	332	0.991
Guimarães (1988)	VG1	0.055	0.13	0.030	1.230	786	1.058

* Data obtained from the proposed curves given by the set of equations 4, 5 and 6; $\clubsuit$Data obtained with rigid plastic analysis (Burgoyne et.al, 1996; Campos, 1999); Fps (exp.)= experimental value for the force in prestressing tendon at ultimate obtained with rigid plastic analysis.

CONCLUSIONS

A numerical parametrical study of the flexural resistance of isostatic concrete beams prestressed with external parallel-lay aramid ropes was carried out. The main variables were the span-depth ratio, total reinforcement index, concrete strength, initial prestressing stress, modulus of elasticity of prestressing tendon, cross-sectional shape and type of loading.

1. Numerical results highlighted the effects of eccentricity variation of the tendons, which led to a reduction in load carrying capacity of the beams. This second order effect should be prevented.

2. As confirmed by experimental results, despite the difference in the prestressing material, the overall behaviour of beams prestressed with external tendons have the same pattern, with final failure occurring by concrete crushing in the compression zone at a particular section.

3. The relative position of the neutral axis (ξ) depends directly on the total reinforcement index (ω_t) defined in this work. The latter parameter was defined from the equilibrium equation between compression and tension forces at a critical section. The neutral axis position was found to be affected by the elastic modulus of the tendons, the depth decreasing as the elastic modulus decreased. Regression curves were obtained between these two parameters.

4. Curves relating rotation capacity and relative position of neutral axis were proposed and, as expected, were influenced by the span-depth ratio. These curves are valid when third point loads are considered.

5. In the ultimate analysis of beams prestressed with unbonded tendons, rotation capacity and depth of neutral axis are unknown variables. The proposed curves gave a good approximation of these two parameters, which could be used in a rigid plastic analysis proposed by the authors in previous works to predict the ultimate force in unbonded prestressing tendons. Although some adjustments need to be made, good agreement was observed between experimental and numerical data.

6. The equations proposed in this work are valid for isostatic beams under third point loads. The analysis is currently being extended in order to cover more complex cases.

ACKNOWLEDGEMENTS

The authors wish to acknowledge the financial assistance provided by CNPq – Conselho Nacional de Desenvolvimento Científico e Tecnológico – Brazil, and The British Council.

REFERENCES

Araújo, A.F. (1997), "Experimental study on the flexural resistance of beams prestressed with external parallel-lay ropes", M.Sc. Thesis, Dept. of Civil Engineering, PUC-Rio, March, 116pp., *in Portuguese.*

Branco, M.M.C. (1993), "Flexural resistance of isostatic beams prestressed with external synthetic tendons", M.Sc. Thesis, Dept. of Civil Engineering, PUC-Rio, October, 56pp., *in Portuguese.*

Burgoyne, C. J., Campos, C. M. O., Guimarães, G. B. (1996), "Behaviour of beams with external tendons", FIP Symposium on Post-Tensioned Concrete Structures, Sept., pp. 1781-1787.

Burgoyne C.J., Guimarães, G.B and Chambers, J.J (1991), "Tests on beams prestressed with unbonded polyaramid tendons", Technical report No. CUED/D, Struct/TR 132, Department of Engineering, University of Cambridge, 38pp.

Campos, C.M.O.(1999), "Analysis of the flexural behaviour of concrete beams prestressed with external synthetic tendons", Ph.D. Thesis, Dept. of Civil Engineering, PUC-Rio, June, 250pp. *in Portuguese.*

CEB-FIP Model Code 1990, Comite Euro-International Du Beton, Lausanne.

Formagini, S. (1999), "Influence of concrete strength on the flexural behaviour of beams prestressed with syntetic tendons", M.Sc. Thesis, Dept. of Civil Engineering, PUC-Rio, August, 85 pp., *in Portuguese.*

Guimarães, G. B. (1988), "Parallel-lay Aramid Ropes for Use in Structural Engineering". Ph.D. Thesis, Imperial College of Science and Technology, Dept. of Civil Engineering, November, 215 pp.

Hillerborg, A (1990), "Fracture mechanics concepts applied to moment capacity and rotational capacity of reinforced concrete beams", Engineering Fracture Mechanics, Vol.35, No.1/2/34, pp. 233-240.

Kherkof, van de K. (1998), "Advanced fibre prestressing", Concrete for the Construction Industry, Vol. 32, Nº 10, November/December, pp. 18-19.

Tan, K.H., Ng, C.K. (1997), "Effects of deviators and tendon configuration on behaviour of externally prestressed beams", ACI Structural Journal, Vol. 94, No.1, January/February, pp.13-22.